JACS
JOURNAL OF THE AMERICAN CHEMICAL SOCIETY

Article

pubs.acs.org/JACS

Structural Melting of an Amino Acid Dimer upon Intersystem Crossing

Ulrich J. Lorenz† and Thomas R. Rizzo*

Laboratoire de Chimie Physique Moléculaire, École Polytechnique Fédérale de Lausanne, CH-1015 Lausanne, Switzerland

ABSTRACT: We present a spectroscopic investigation of the excited-state dynamics of the phenylalanine (Phe)/serine (Ser) protonated dimer in the gas phase. Using an ultraviolet (UV) laser pulse, we promote individual isomers to the S_1 state and probe their fate with an infrared (IR) pulse. We find that the S_1 state has a lifetime of ∼70 ns and undergoes intersystem crossing (ISC) to the T_1 state. Time-resolved IR spectra allow us to follow the structural evolution of the dimer. In the S_1 state, the different isomers retain the hydrogen-bonding pattern of the ground state. Intersystem crossing triggers a sudden increase of the vibrational energy, so that the dimers can overcome isomerization barriers and explore large parts of the potential energy surface (PES). Their broad IR spectra largely resemble one another and indicate that the dimers adopt a molten structure.

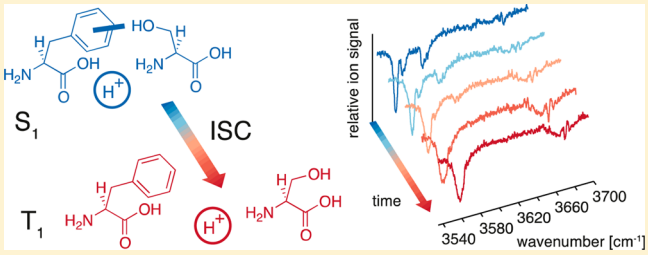

1. INTRODUCTION

The structure and function of proteins are determined by a limited number of molecular-level interactions whose nature is well understood individually, such as the formation of hydrogen bonds, electrostatic and dispersive forces, or hydrophobicity. Yet, the multitude of possible interactions, even in systems of moderate size, results in an overwhelming complexity, making the prediction of protein structure or the design of specific functions a formidable task. The concept of the potential energy surface (PES) provides a tool to understand this complexity in terms of local minima, which represent stable configurations, and saddle points that separate them from each other.[1] Characterizing these stationary points of the PES experimentally is challenging. However, by isolating biomolecules from the solvent and transferring them to the gas phase, small systems can be made tractable, so that detailed insights into the properties of the PES can be gained. In particular, investigations of cold biomolecules in the gas phase by means of IR/UV and UV/UV double resonance techniques have been able to identify different stable conformers, and their structures have been elucidated with the help of quantum chemical calculations.[2−10] Moreover, population transfer spectroscopy has made it possible to probe the interconversion of these conformers and to obtain the associated barrier heights and quantum yields.[11−14] These studies provide fundamental insights into the intrinsic properties of the PES of biomolecules and may help to verify and calibrate computational tools.

We have previously demonstrated that the Phe/Ser protonated dimer[15] shows a complex intermolecular interaction that leads to the simultaneous presence of at least five different isomers. In three of them (isomers A, B, and C in the terminology of ref 15), the amino group of the more basic amino acid Phe is protonated, whereas, in the remaining two (D, E), the Ser amino group carries the excess proton. Here, we extend these investigations to interrogate the evolution of the dimer structure following electronic excitation, which allows us to gain further insight into the properties of the PES. Moreover, we investigate the excited-state dynamics of the dimer, which emulate the solution-phase photochemistry of Phe containing proteins[16] in a more tractable gas phase experiment. Our experimental approach is related to various UV pump/IR probe schemes, including ultrafast techniques,[17−22] but resembles most closely a method that has previously been used to obtain the excited-state IR spectra of neutrals.[23,24] The latter technique exploits the change in the fluorescence quantum yield of an excited-state species upon absorption of an IR photon. Here, we monitor the photofragmentation yield instead and are therefore not limited to fluorescing species. Moreover, we can distinguish species in different electronic states by their different fragmentation patterns, allowing us to record selective IR spectra of the S_0, S_1, and T_1 states of the dimers. Furthermore, we elucidate the excited-state dynamics of the dimer and the role of different competing photofragmentation mechanisms. Intersystem crossing leads to a sudden increase of the vibrational energy of the dimers, allowing them to overcome isomerization barriers and interconvert, a process that has not been observed in smaller systems and provides access to studying conformational dynamics at high vibrational energies. The melting of the dimer structure upon ISC manifests itself in the evolution of the IR spectroscopic signature, which we follow in real time.

2. EXPERIMENTAL APPROACH

We prepare the Phe/Ser protonated dimers at ∼10 K[25] as previously determined in our investigation of their ground electronic state.[15]

Received: August 4, 2014
Published: September 24, 2014

   dx.doi.org/10.1021/ja507981p | J. Am. Chem. Soc. 2014, 136, 14974−14980

Briefly, the protonated 1:1 clusters of L-Phe and L-Ser are generated by nanoelectrospray from a 100 μM/1 mM methanol/water (1:1) solution. They are pretrapped in a storage hexapole, mass-selected with a quadrupole mass analyzer, and injected into a cryogenic 22-pole ion trap, where they are cooled in collisions with helium. The ions are irradiated with a UV laser pulse, ejected from the trap, and mass analyzed with a second quadrupole filter. We obtain a UV spectrum by detecting the occurrence of photofragments as a function of the laser wavenumber. To record an IR spectrum of the ground state, we fix the UV laser to the transition of a specific isomer and fire the IR laser ~30 ns prior to the UV laser pulse. If the IR frequency is in resonance with a vibrational transition, it removes population from the ground state and thus depletes the fragment ion signal. An IR spectrum is obtained by recording the depletion as a function of the IR wavenumber.

We reverse the sequence of the laser pulses in order to obtain isomer-specific IR spectra in the excited state. If the electronically excited species absorbs an IR photon, its fragmentation pattern changes, which we illustrate through difference mass spectra (*DifferenceMS*) according to the expression

$$Difference\ MS = UVIR - UV - (IR - No\ Laser)$$

where *UVIR*, *UV*, *IR*, and *No Laser* denote mass spectra recorded with both the UV and IR laser, only the UV laser, only the IR laser, and without any laser, respectively. It is necessary to subtract the term in brackets to eliminate a background signal arising from the action of the IR laser alone. This signal appears predominantly in the m/z 166 mass channel and is probably due to a broad IR absorption of larger, multiply charged clusters that are present under our experimental conditions. We obtain the IR spectrum of a species in its excited state by monitoring the enhancement or depletion of a fragment mass channel as a function of the IR wavenumber. The delay between the laser pulses is chosen such that they do not overlap in time. Processes in which IR absorption precedes UV excitation therefore cannot occur and contribute to the spectra.

3. RESULTS AND DISCUSSION

3.1. UV photofragment spectra. As previously reported,[15] UV excitation of the protonated dimer (Phe·SerH$^+$) leads to the creation of several photofragments (Figure 1(a)). Protonated serine (SerH$^+$) and protonated phenylalanine (PheH$^+$) are observed as well as fragments with m/z 180 (loss of the Phe side chain) and m/z 120 (loss of Ser, H_2O, and CO).

We have previously established that the UV photofragment spectrum (Figure 2, recorded by monitoring the 180 amu channel) contains contributions from at least five different conformational isomers with distinct IR spectra. In the following, we present our investigation of the excited-state properties of isomers A, B, and E (nomenclature of ref 15), for which the best signal-to-noise levels could be achieved, and note that isomers C and D exhibit analogous behavior. We prepare the excited states by pumping the UV transitions of isomers A, B, and E that are marked in Figure 2. For isomer A, either the band origin (37596.1 cm^{-1}) or a vibronic band (38128.7 cm^{-1}, 532.6 cm^{-1} above the band origin) is used. Isomer B is pumped at its band origin (37613.7 cm^{-1}) and isomer E at 38432.8 cm^{-1} (529.6 cm^{-1} above its band origin).

3.2. Infrared spectra of the S_1 state. The photofragment mass spectrum of isomer A (Figure 1(a)) changes when the ions are irradiated with an IR laser pulse (3558 cm^{-1}) that follows the UV laser pulse at a delay of 20 ns. This is apparent in the difference mass spectrum of Figure 1(b). The positive peaks at m/z 120 and 166 indicate that the corresponding fragment channels are enhanced by the action of the IR laser, and the negative peak at m/z 180 that this channel is depleted.

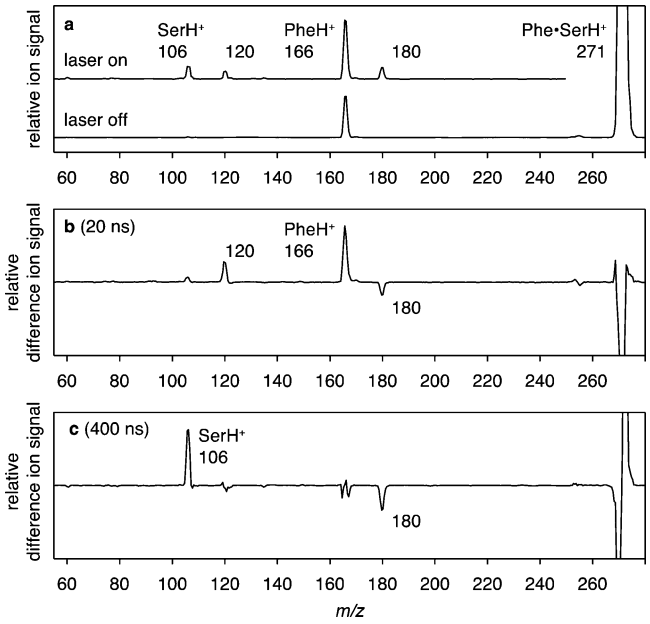

Figure 1. (a) Fragment mass spectra of Phe·SerH$^+$ obtained without UV laser ("laser off") and after UV irradiation at 37596.1 cm^{-1}; the band origin of isomer A in the terminology of ref 15 ("laser on"). (b and c) Difference mass spectra showing the enhancement (positive peaks) and depletion (negative peaks) of different mass channels that result when the UV-excited species (isomer A) is irradiated with an IR laser pulse. The IR laser was tuned to 3558 cm^{-1}, and the IR pulse followed the UV laser pulse at a delay of 20 and 400 ns in parts b and c, respectively.

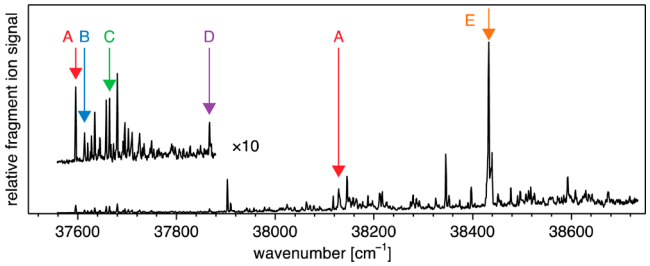

Figure 2. UV photofragment spectrum of the protonated dimer in the 180 amu mass channel.

Similar difference mass spectra were also observed for the other isomers.

By monitoring the enhancement of the 120 amu channel while scanning the IR laser (fired 20 ns after the UV laser), we obtain IR spectra of isomers A, B, and E in the S_1 state. Figure 3 compares them with the previously reported ground-state IR depletion spectra (top traces); the shading indicates the spectral ranges of different hydride stretch vibrations. We first discuss the excited-state vibrational spectrum of isomer A labeled "S_1, band origin", which was obtained after UV excitation of isomer A at its band origin. It bears resemblance to the spectrum in S_0 but shows lower intensities in the CH and NH stretch ranges. In the excited state, the two carboxylic acid OH stretch bands as well as the bands of the NH_2 group experience a small red-shift of ~3 cm^{-1} and ~2 cm^{-1}, respectively. In the NH_3^+ range, only the position of the most intense band can be determined, which features a red-shift of ~7 cm^{-1}. We have previously proposed[15] that, in isomer A, the OH group of the Ser side chain engages in a π-hydrogen

dx.doi.org/10.1021/ja507981p | J. Am. Chem. Soc. 2014, 136, 14974−14980

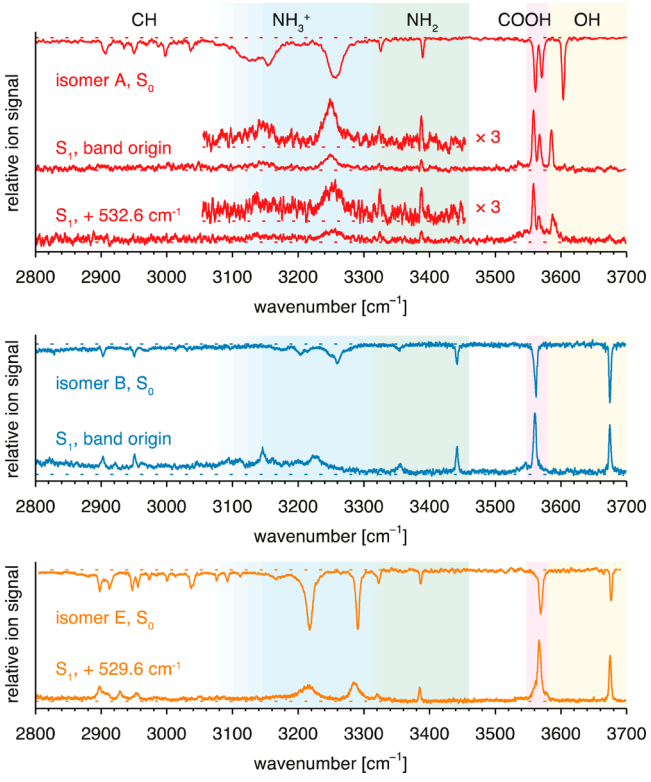

Figure 3. Ground-state IR spectra of isomers A, B, and E (top traces) and IR spectra in S_1, recorded in the 120 amu channel with a delay of 20 ns between the UV and IR laser pulses. The S_1 state of isomer A was prepared by either pumping the band origin or a vibronic band at 532.6 cm^{-1} above the band origin. Isomer B was excited at the band origin and isomer E with an excess energy corresponding to 529.6 cm^{-1}. The shading indicates the spectral ranges of the hydride stretches.

bond with the aromatic ring. Upon electronic excitation, this OH stretch vibration undergoes a further red-shift of ~18 cm^{-1}, supporting our earlier assignment and indicating that the strength of the π-hydrogen bond increases in S_1.

Since the ground and excited states feature similar band positions for the NH and OH stretches, we infer that both electronic states possess the same hydrogen-bond pattern and structure. Moreover, the almost identical widths of the IR bands in both spectra indicate that the excited-state species is vibrationally cold, supporting our assignment to the S_1 state. If a radiationless transition to a different electronic state had occurred, the widths of the vibrational bands should reflect the resulting high vibrational energy, which is not consistent with our findings. It can be demonstrated that the width of the IR bands is a sensitive probe of the vibrational energy of the dimer when the S_1 state of isomer A is prepared with an excess energy corresponding to 532.6 cm^{-1} (Figure 3). Most notably, the width of the most intense NH_3^+ band increases by ~10 cm^{-1}, the OH stretch band of the Ser side chain develops a shoulder at higher photon energies and increases in width by ~3 cm^{-1}, and a broad background appears in the range of the OH stretch peaks. The increase of the line width likely results from a combination of two effects.[26] At high internal energy, a large number of low frequency modes is significantly populated. The vibrational wave function is a superposition of different eigenstates of the same energy, each of them shifting the frequency of the IR transition by a different amount that depends on the strength of the intermode anharmonic coupling. This so-called "statistical inhomogeneous broadening"[26] of the IR band becomes more important at higher internal energy, where a larger number of states contribute to the superposition. The vibrational bands can also be homogeneously broadened through coupling of the excited "bright state" to nearby "dark states", resulting in a large number of close-lying eigenstates with partial "bright-state" character. At elevated internal energy where the density of states is higher, more eigenstates in a wider energy range may be involved that can be excited in transitions from a single energy level, leading to an increased line width. This is simply the frequency domain manifestation of intramolecular vibrational energy redistribution (IVR).

Our analysis of the IR spectrum of the S_1 state of isomer B, prepared by pumping the band origin, follows a similar line of argument. In the range of the NH_2 and OH vibrations, the spectrum is almost identical to the spectrum of the ground state, consistent with an internally cold species that possesses the same structure as the ground state. The NH_3^+ vibrations, however, appear red-shifted and show a different spectral signature, possibly indicating a change in the interaction between the ammonium group and the aromatic ring. In contrast to isomer A, the CH stretch range of isomer B shows clearly discernible peaks. For isomer E, whose excited state was prepared with an excess energy corresponding to 529.6 cm^{-1}, small red-shifts of the NH and OH stretch bands are observed (2−4 cm^{-1}) together with a considerable broadening of the NH_3^+ bands. This indicates that the excited cluster possesses the same hydrogen-bond pattern as the ground state but has a higher vibrational energy. The spectral signature of the CH range clearly differs from that in the ground state, possibly pointing to slight conformational changes in the excited state that do not involve the hydrogen-bond network.

3.3. Infrared spectra of the T_1 state. When the delay between the UV pump and the IR probe pulses is increased from 20 to 400 ns, the photofragmentation pattern of isomer A changes (Figure 1(c)), indicating that a different species is being observed. The difference mass spectrum shows depletion of the m/z 180 fragment and enhancement of $SerH^+$ (m/z 106). In contrast, the yield of $PheH^+$ (m/z 166) remains unchanged. This fragment corresponds to intermolecular dissociation, with the excess proton remaining on Phe, whose proton affinity is more than 8 kJ/mol higher than that of Ser.[27,28] Since this channel is the energetically most favorable in S_0 but is not enhanced upon IR absorption, we infer that the observed species is not in the electronic ground state. Instead, we identify it with the T_1 state. This assignment is consistent with the high vibrational energy of the species, and its transient signal and is furthermore supported by the known photochemistry of related compounds and their similar fragmentation behavior, as we will discuss below.

Structural information about the T_1 state can be obtained from its IR spectra, which we recorded by firing the IR laser 400 ns after the UV laser and monitoring the 180 amu channel (Figure 4). The spectra of isomers A, B, and E are almost identical to one another. The sharp spectral features of the S_1 state are absent, indicating that it does not contribute. Instead, a broad and weak absorption is observed that spans the CH and NH stretch ranges. The carboxylic acid OH stretches appear as a broad, red-shifted feature centered around 3557 cm^{-1} with a width of ~10 cm^{-1}, while in S_0, they are observed between 3561 and 3569 cm^{-1} with a width of only ~6 cm^{-1}. The Ser

dx.doi.org/10.1021/ja507981p | J. Am. Chem. Soc. 2014, 136, 14974−14980

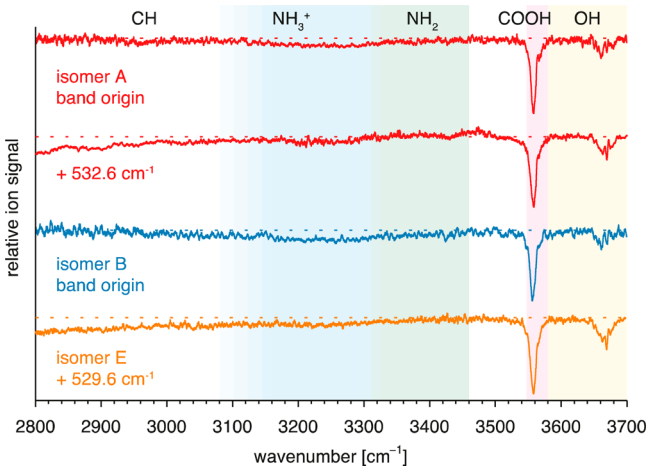

Figure 4. Infrared spectra of the T_1 state of isomers A, B, and E, recorded in the 180 amu channel with a delay of 400 ns between the UV and IR laser pulses. The T_1 state of isomer A was prepared by either pumping the band origin or a vibronic band 532.6 cm^{-1} above the band origin. Isomer B was excited at the band origin and isomer E with an excess energy corresponding to 529.6 cm^{-1}. The shading indicates the spectral ranges of the hydride stretches.

OH stretch band appears at 3666 cm^{-1}, indicating a free OH group that is not involved in a hydrogen bond. The band is red-shifted relative to the free OH bands of isomers B and E in S_0 (3674 and 3677 cm^{-1}, respectively) and considerably broadened to a width of ~20 cm^{-1} (compared to ~3 cm^{-1} in S_0). It should be noted that the structure observed on top of the band is due to water absorption in the IR beam path that we could not remove completely by power normalization.

These spectral features, and in particular the red-shift and broadening of the absorption bands, indicate a high vibrational energy, as expected for a species that has undergone ISC. The broadening is most pronounced for the NH stretch bands, which frequently also appear broad in the room temperature IR spectra of protonated amino acid dimers.[29−31] In isomer A, the π-hydrogen bond of the Ser OH group is broken and a free OH band is observed. The fact that all isomers show closely similar IR spectra in T_1 despite their different spectra and structures in S_0 (and S_1) suggests that their vibrational energy in the T_1 state is sufficiently high for them to overcome isomerization barriers and interconvert. It should also be noted that, in isomers A and B, isotopic substitution studies have shown that the excess proton is located on Phe, while, in E, it is located on the less basic amino acid Ser.[15] Interconversion between these isomers must therefore involve proton transfer. The S_1-T_1 gap of the dimers can be estimated from that of toluene to be on the order of 100 kJ/mol (corresponding to ~8400 cm^{-1}),[32,33] which is below the typical dissociation energy of protonated amino acid dimers (on the order of 110−130 kJ/mol[34−36]) but well above typical thresholds for conformational isomerization of simple organic molecules (around 12 kJ/mol[12,37]). It can thus be expected that the dimers are sufficiently hot to explore large parts of the T_1 PES. The simultaneous presence of different isomers with different spectral signatures may further increase the width of the IR bands, adding to the line broadening that results at high internal energy due to the mechanisms discussed above. The similar broad spectral signature that the different isomers exhibit and the loss of specific hydrogen-bond interactions such as the π-hydrogen bond of isomer A, together with the energetics of ISC and conformational isomerization, lead us to conclude that the T_1 state adopts a fluctuating structure that could best be described as "molten", in contrast to the distinct "frozen out" structures that the dimer adopts at low internal energy.

Close inspection of the IR spectra in T_1 reveals that the carboxylic acid OH stretch bands of different isomers have slightly different peak shapes and positions (Figure 5). This

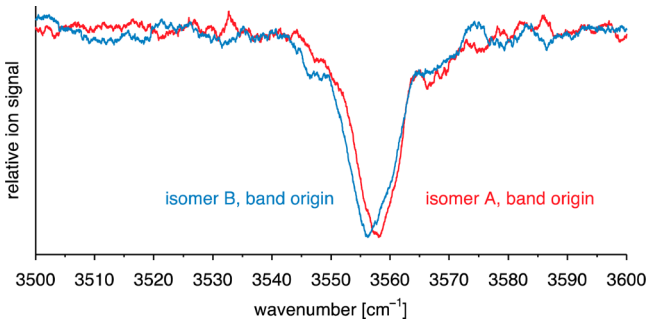

Figure 5. Infrared spectra of the T_1 state of isomers A and B in the region of the carboxylic acid OH stretch band, recorded in the 180 amu channel with a delay of 400 ns between the UV and IR laser pulses. The spectra were acquired under identical conditions and calibrated using water absorptions in the IR beam path. A reproducible, relative difference in the carboxylic acid OH stretch peak of ~2 cm^{-1} is observed. The T_1 states of isomers A and B were prepared by pumping their respective band origins.

suggests that excitation of different ground-state isomers leads to different ensembles of hot triplet species that are separated by sufficiently high barriers on the T_1 surface, so that 400 ns after UV excitation, they have not yet fully interconverted. Despite their high internal energies, they retain a memory of their structure in S_0 and explore different regions of the PES.

3.4. Transient signals of the S_1 and T_1 states. Figure 6 shows the transient signals of the S_1 and T_1 states of isomer E,

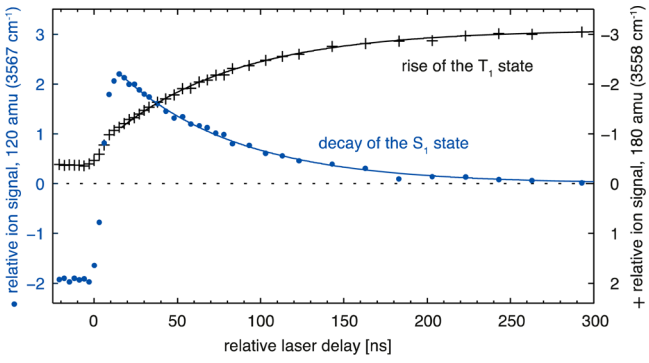

Figure 6. Transient signals of the S_1 and T_1 states of isomer E. The population of the S_1 state (blue dots) is probed by IR excitation of its carboxylic acid OH stretch band (3567 cm^{-1}) and monitoring the resulting enhancement of the 120 amu fragment. The population of the T_1 state (black crosses) is probed by exciting its carboxylic acid OH stretch (3558 cm^{-1}), which leads to the depletion of the 180 amu fragment.

for which we could obtain the best signal-to-noise ratio. The population in the S_1 state (blue dots) is monitored by exciting its carboxylic acid OH stretch band with the IR probe pulse (3567 cm^{-1}) and thereby enhancing the 120 amu fragment (see Figure 1(b)). At negative time delays (i.e., the IR probe precedes the UV pump), this fragment channel is depleted due

dx.doi.org/10.1021/ja507981p | J. Am. Chem. Soc. 2014, 136, 14974−14980

to the IR absorption of S_0. At positive times, the buildup and subsequent decay of the S_1 state can be observed. We monitor the population in the T_1 state (black crosses) by pumping its carboxylic acid stretch band (3558 cm^{-1}), which depletes the 180 amu channel (Figure 1(c)); the depletion signal is plotted in the positive direction. The signal at negative times originates from IR absorption of the ground state, while, at positive times, the rise of the T_1 population can be observed. Exponential fits (solid lines) yield similar time constants for the lifetime of S_1 (71 ± 3 ns) and the rise time of T_1 (75 ± 4 ns), consistent with our interpretation that we are observing ISC between the S_1 and T_1 states. Similar time constants were also determined for the other isomers (Table 1). We note that the determination of the population in S_1 and T_1 by probing at a fixed wavelength assumes that the position and width of the COOH stretch bands do not evolve over time, which could otherwise distort the measured transient. This is certainly the case for the S_1 species, with IVR being much faster than the time scale we are probing. In contrast, conformational isomerization of the T_1 species could potentially be much slower. However, since we obtain roughly the same time scale for the decay of S_1 and the rise of T_1, we can conclude that such effects play a minor role and cannot significantly affect the measurement.

Table 1. Measured Lifetimes of the S_1 State and Rise Times of the T_1 State[a]

	Lifetime of S_1 [ns]	Rise time of T_1 [ns]
Isomer A (band origin)	59 ± 12	47 ± 5
Isomer A (+532.6 cm^{-1})	63 ± 8	52 ± 11
Isomer B (band origin)	110 ± 62	61 ± 32
Isomer E (+529.6 cm^{-1})	71 ± 3	75 ± 4

[a]For isomer A, either the band origin or the vibronic band at 532.6 cm^{-1} above the band origin was pumped to prepare the excited state.

Our experiments show that the T_1 state has a lifetime of at least 100 μs. A more precise determination of this lifetime meets several challenges. After the UV pump pulse, the excited ions leave the volume of the UV laser beam and redistribute over the entire volume of the 22-pole trap.[38] While this redistribution is not fast enough to affect the determination of the short S_1 lifetime, it complicates the analysis for much slower processes. Moreover, for such long time scales, collisions with the buffer gas become important. However, we can conclude that the long lifetime is consistent with a triplet species.

3.5. Time-resolved IR spectra. The IR spectra of the S_1 state in Figure 3 were recorded by monitoring the m/z 120 fragment in order to discriminate against the triplet species, whose spectrum cannot be obtained in this channel (see Figure 1). However, the S_1 and T_1 states can be observed simultaneously in the 180 amu channel, which is depleted when either species absorbs an IR photon. This is shown in the time-resolved IR spectra of isomer A in Figure 7, which capture the evolution of the entire system following UV excitation of the vibronic band.

The IR spectra initially show the sharp spectral signature of the vibrationally cold S_1 state. As the ensemble undergoes ISC, the two narrow transitions in the carboxylic acid OH stretch range are gradually replaced by the broad and red-shifted absorption that is characteristic of the internally hot T_1 state. Upon ISC, the vibrational energy suddenly increases and the protonated dimer adopts a molten structure that is characterized by rapid interconversion between the different local minima of the free energy surface. The melting process is vividly illustrated by the evolution of the Ser OH stretch band. It undergoes a blue shift and appears as a broad feature in the spectral region characteristic of a free OH oscillator, indicating that the π-hydrogen bond of the OH group that stabilizes the S_1 state is broken as the dimer melts. More than 400 ns after the UV pulse, the signature of the S_1 state has completely vanished from the IR spectrum.

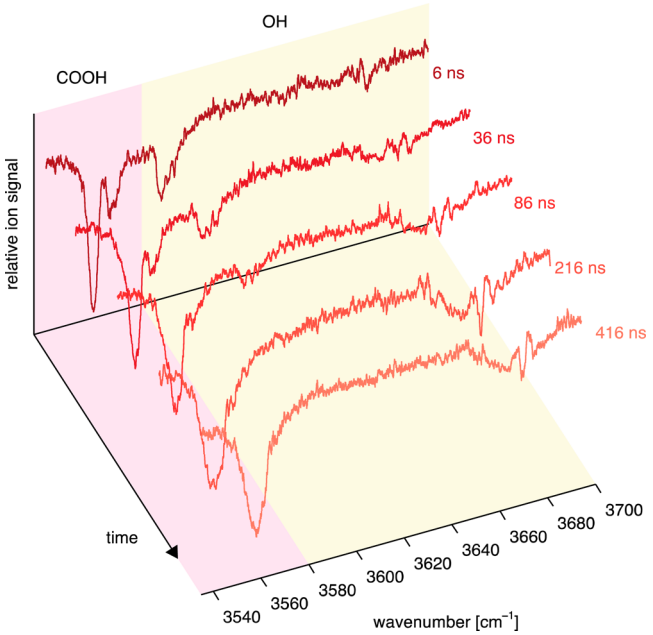

Figure 7. Infrared spectra of isomer A, recorded at various delays after UV excitation of the vibronic band. The 180 amu fragment channel is being monitored, so that the S_1 and T_1 states can be observed simultaneously. The shading indicates the spectral ranges of the hydride stretches.

3.6. Mechanistic considerations. Our analysis of the excited-state dynamics of the Phe/Ser protonated dimer is supported by the known photochemistry of Phe and Phe analogs in solution and in the gas phase. In neutral and acidic aqueous solution at room temperature, Phe has a fluorescence lifetime of ~5−7 ns[39,40] and undergoes ISC with a quantum yield of 0.4[16] to the T_1 state, which has a lifetime of ~2−3 μs.[41] The T_1 state was identified as the precursor for the dissociation of the $C_α$-$C_β$ bond under formation of a benzyl radical, the same neutral fragment that accompanies the m/z 180 photofragment ion of the protonated Phe/Ser dimer. In the gas phase, different conformers of jet-cooled, neutral Phe were found to have S_1 lifetimes of ~70−90 ns,[42] very close to the lifetimes obtained for the protonated dimers. Only one Phe conformer forms an exception, with a considerably shorter lifetime of 29 ns.[42] More ample data are available on the excited-state dynamics of simpler alkylbenzenes. Toluene, when excited near the band origin, has an S_1 lifetime of about 70−80 ns,[43,44] undergoes ISC with a quantum yield of 0.64,[45,46] and has a T_1 lifetime of about 3 μs.[46,47] For ethylbenzene, a fluorescence lifetime of 80 ns[48] and a T_1 lifetime of 2.5 μs[47] have been measured when the excitation wavelength was 266 nm. After 248 nm excitation, ethylbenzene and *n*-propylbenzene both dissociate via formation of the benzyl radical.[49,50] Photofragment translational spectroscopy revealed that 75−80% of the benzyl fragments originate from dissociation in an excited electronic state, and *ab initio* calculations suggest that

dx.doi.org/10.1021/ja507981p | J. Am. Chem. Soc. 2014, 136, 14974−14980

this excited state is the T_1 state.[49] It was inferred that ethylbenzene and *n*-propylbenzene possess high ISC quantum yields of over 0.75−0.8.[49] The same dissociation mechanism was also found to operate for the isomeric ethyltoluenes[50] and, most importantly, for small Phe model compounds.[51] For the latter, quantum chemical calculations predict dissociation barriers on the T_1 surface of about 20−40 kJ/mol, while the dissociation energy in S_0 is on the order of 200 kJ/mol.[51] For comparison, intermolecular dissociation of a protonated amino acid dimer in the ground state requires only about 110−130 kJ/mol.[34−36] We conclude that the 180 amu fragment is not formed in S_0,[52] but predominantly arises from dissociation in T_1. This is also supported by recent work from our laboratory on the protonated peptide Ac-FA_5K, which shows clear evidence for benzyl radical formation from the T_1 state.[53]

The excited-state dynamics of Phe and the alkylbenzenes are largely dominated by the properties of the benzyl chromophore. It is therefore not surprising that the Phe/Ser protonated dimer shows a similar excited-state chemistry. The analogies between the existing body of information and our own findings support our analysis, which we summarize in the following. Upon UV excitation, we prepare the S_1 state of the protonated dimer, which has a lifetime of about 70 ns and undergoes ISC to the T_1 state. The hot triplet species predominantly fragments through dissociation of the C_α-C_β bond to give the 180 amu fragment, a process that is associated with an activation barrier on the T_1 surface. The T_1 lifetime of over 100 μs that we observe is considerably longer than that of related neutral species. Absorption of an IR photon of the T_1 species depletes the 180 amu channel and enhances the 106 amu channel. The *m*/*z* 106 fragment ($SerH^+$) must originate from a process occurring on an excited-state surface, since dissociation in S_0 should predominantly yield the most stable product of intermolecular dissociation, $PheH^+$, which is not enhanced upon IR absorption. We therefore conclude that the change in fragmentation pattern results from the competition between two excited-state dissociation channels and that, at higher vibrational energies, dissociation in the 106 amu channel becomes more efficient. It should also be noted that the 106 amu fragment channel, which corresponds to intermolecular dissociation with the proton on Ser, is not available for covalently bound molecules and is therefore specific for the protonated amino acid dimer studied here.

Infrared excitation of the S_1 state leads to depletion of the *m*/*z* 180 fragment, which predominantly originates from dissociation in T_1, as discussed above. At the same time, the *m*/*z* 166 and 120 channels are enhanced, which we both ascribe to ground-state dissociation processes. As pointed out above, the *m*/*z* 166 fragment channel possesses the lowest dissociation energy in S_0, while the 120 amu ion (loss of H_2O and CO from $PheH^+$) is the most abundant fragment created through collision induced dissociation (CID) of ground-state $PheH^+$.[54] The simultaneous enhancement of both fragments therefore strongly suggests that they are formed in S_0 following internal conversion (IC). Apparently, IR absorption decreases the ISC quantum yield while increasing the efficiency of IC. This resembles the "channel 3" behavior of benzene, which shows rapid, nonradiative relaxation when excited to levels ≥3000 cm^{-1} above the band origin. A widely accepted explanation for this effect is that a "third channel" (besides fluorescence and ISC) becomes accessible at these energies that involves rapid IC to the ground electronic state through a conical intersection.[55] Toluene exhibits a similar decrease of the fluorescence lifetime and quantum yield with increasing excitation energy. This behavior has been linked to the "channel 3" effect and already sets in ≥2000 cm^{-1} above the band origin.[43,44] It therefore appears plausible that "channel 3" behavior could explain the change in fragmentation pattern that occurs when the S_1 state of the protonated dimers absorbs an IR photon of ≥2800 cm^{-1}.

4. CONCLUSIONS

The experimental approach presented here allows us to prepare and probe the vibrationally cold S_1 state of a specific isomer of the Phe/Ser protonated dimer. Higher amounts of vibrational energy can be deposited in the molecule when a suitable vibronic band is selected for UV excitation. If we do so, we find that the width of the NH_3^+ vibrations and the π-hydrogen-bonded OH stretch vibration of isomer A are a sensitive probe of the internal energy of the dimer. The IR spectra of the S_1 state indicate the same hydrogen-bond pattern as in the ground state. However, it should also be possible to induce structural isomerization at higher UV excitation energies and implement an excited-state analog of population transfer spectroscopy.

Using a UV pump/IR probe scheme, we can follow the fate of the excited species. We find that the S_1 state has a lifetime of ∼70 ns and undergoes intersystem crossing (ISC) to the T_1 state, which possesses a lifetime of >100 μs. Infrared excitation of either species induces different changes of the fragmentation pattern. This allows us to obtain selective IR spectra of either electronic state or IR spectra that show both species simultaneously. We interpret the change in fragmentation pattern of the S_1 species in terms of an increase of the IC and a decrease of the ISC quantum yield, which is possibly linked to the "channel 3" behavior of the benzene chromophore. For the T_1 state, we conclude that IR excitation changes the branching ratio between two competing excited-state dissociation channels.

The IR spectra of the T_1 state of different ground-state isomers are similar to each other and show broad, red-shifted features, indicating a high vibrational energy. We conclude that the T_1 species has sufficient vibrational energy to overcome isomerization barriers and explore large parts of the PES. Subtle differences between the T_1 spectra of different ground-state isomers reveal that the randomization of the structure on the T_1 PES is not complete. It would be interesting to investigate whether further information about the isomerization of the T_1 species could be gained from the evolution of the IR spectra.

Time-resolved IR spectra allow us to follow the structural transformation of the protonated dimer in real time. Intersystem crossing triggers a sudden increase of the vibrational energy of the dimer and causes the melting of its structure. This is most vividly illustrated by the IR spectra of isomer A. Upon melting, the π-hydrogen bond that stabilizes this isomer at low internal energies is broken.

■ AUTHOR INFORMATION

Corresponding Author

*thomas.rizzo@epfl.ch

Present Address

[†](U.J.L.) California Institute of Technology, Pasadena, CA 91125, USA.

Notes

The authors declare no competing financial interest.

■ ACKNOWLEDGMENTS

We gratefully acknowledge financial support for this work from the Fonds National Suisse (through Grant Nos. 200020-130579 and 206021-117416) and the Ecole Polytechnique Fédérale de Lausanne (EPFL). U.J.L. is thankful for a doctoral fellowship from the "Fonds der Chemischen Industrie" of Germany.

■ REFERENCES

(1) Wales, D. J.; Bogdan, T. V. *J. Phys. Chem. B* **2006**, *110*, 20765.
(2) Chin, W.; Compagnon, I.; Dognon, J. P.; Canuel, C.; Piuzzi, F.; Dimicoli, I.; von Helden, G.; Meijer, G.; Mons, M. *J. Am. Chem. Soc.* **2005**, *127*, 1388.
(3) Gerhards, M.; Unterberg, C.; Gerlach, A.; Jansen, A. *Phys. Chem. Chem. Phys.* **2004**, *6*, 2682.
(4) Bakker, J.; Plutzer, C.; Hunig, I.; Haber, T.; Compagnon, I.; von Helden, G.; Meijer, G.; Kleinermanns, K. *ChemPhysChem* **2005**, *6*, 120.
(5) Bakker, J. M.; Aleese, L. M.; Meijer, G.; von Helden, G. *Phys. Rev. Lett.* **2003**, *91*, 203003.
(6) de Vries, M. S.; Hobza, P. *Annu. Rev. Phys. Chem.* **2007**, *58*, 585.
(7) Florio, G. M.; Zwier, T. S. *J. Phys. Chem. A* **2003**, *107*, 974.
(8) Robertson, E. G.; Simons, J. P. *Phys. Chem. Chem. Phys.* **2001**, *3*, 1.
(9) Inokuchi, Y.; Kobayashi, Y.; Ito, T.; Ebata, T. *J. Phys. Chem. A* **2007**, *111*, 3209.
(10) Rizzo, T. R.; Stearns, J. A.; Boyarkin, O. V. *Int. Rev. Phys. Chem.* **2009**, *28*, 481.
(11) Dian, B. C.; Longarte, A.; Zwier, T. S. *Science* **2002**, *296*, 2369.
(12) Dian, B. C.; Clarkson, J. R.; Zwier, T. S. *Science* **2004**, *303*, 1169.
(13) Dian, B. C.; Florio, G. M.; Clarkson, J. R.; Longarte, A.; Zwier, T. S. *J. Chem. Phys.* **2004**, *120*, 9033.
(14) Dian, B. C.; Longarte, A.; Winter, P. R.; Zwier, T. S. *J. Chem. Phys.* **2004**, *120*, 133.
(15) Lorenz, U. J.; Rizzo, T. R. *J. Am. Chem. Soc.* **2012**, *134*, 11053.
(16) Chin, K. K.; Trevithick-Sutton, C. C.; McCallum, J.; Jockusch, S.; Turro, N. J.; Scaiano, J. C.; Foote, C. S.; Garcia-Garibay, M. A. *J. Am. Chem. Soc.* **2008**, *130*, 6912.
(17) Kang, H.; Dedonder-Lardeux, C.; Jouvet, C.; Gregoire, G.; Desfrancois, C.; Schermann, J. P.; Barat, M.; Fayeton, J. A. *J. Phys. Chem. A* **2005**, *109*, 2417.
(18) Kang, H.; Jouvet, C.; Dedonder-Lardeux, C.; Martrenchard, S.; Gregoire, G.; Desfrancois, C.; Schermann, J.; Barat, M.; Fayeton, J. *Phys. Chem. Chem. Phys.* **2005**, *7*, 394.
(19) Lucas, B.; Barat, M.; Fayeton, J. A.; Perot, M.; Jouvet, C.; Gregoire, G.; Nielsen, S. B. *J. Chem. Phys.* 2008, *128*164302.
(20) Gregoire, G.; Lucas, B.; Barat, M.; Fayeton, J. A.; Dedonder-Lardeux, C.; Jouvet, C. *Eur. Phys. J. D* **2009**, *51*, 109.
(21) Tanabe, K.; Miyazaki, M.; Schmies, M.; Patzer, A.; Schutz, M.; Sekiya, H.; Sakai, M.; Dopfer, O.; Fujii, M. *Angew. Chem., Int. Ed.* **2012**, *51*, 6604.
(22) Fujii, M.; Dopfer, O. *Int. Rev. Phys. Chem.* **2012**, *31*, 131.
(23) Walther, T.; Bitto, H.; Minton, T. K.; Huber, J. R. *Chem. Phys. Lett.* **1994**, *231*, 64.
(24) Dian, B.; Longarte, A.; Zwier, T. *J. Chem. Phys.* **2003**, *118*, 2696.
(25) Svendsen, A.; Lorenz, U. J.; Boyarkin, O. V.; Rizzo, T. R. *Rev. Sci. Instrum.* **2010**, *81*, 073107.
(26) Makarov, A. A.; Petrova, I. Y.; Ryabov, E. A.; Letokhov, V. S. *J. Phys. Chem. A* **1998**, *102*, 1438.
(27) Hunter, E.; Lias, S. *J. Phys. Chem. Ref. Data* **1998**, *27*, 413.
(28) Afonso, C.; Modeste, F.; Breton, P.; Fournier, F.; Tabet, J. *Eur. J. Mass Spectrom.* **2000**, *6*, 443.
(29) Oh, H.; Lin, C.; Hwang, H.; Zhai, H.; Breuker, K.; Zabrouskov, V.; Carpenter, B.; McLafferty, F. *J. Am. Chem. Soc.* **2005**, *127*, 4076.
(30) Kong, X.; Tsai, I.; Sabu, S.; Han, C.; Lee, Y.; Chang, H.; Tu, S.; Kung, A.; Wu, C. *Angew. Chem., Int. Ed.* **2006**, *45*, 4130.
(31) Atkins, C. G.; Rajabi, K.; Gillis, E. A. L.; Fridgen, T. D. *J. Phys. Chem. A* **2008**, *112*, 10220.
(32) Swiderek, P.; Michaud, M.; Sanche, L. *J. Chem. Phys.* **1996**, *105*, 6724.
(33) Bolovinos, A.; Philis, J.; Pantos, E.; Tsekeris, P.; Andritsopoulos, G. *J. Mol. Spectrosc.* **1982**, *94*, 55.
(34) Price, W.; Schnier, P.; Williams, E. *J. Phys. Chem. B* **1997**, *101*, 664.
(35) Raspopov, S.; McMahon, T. *J. Mass Spectrom.* **2005**, *40*, 1536.
(36) Meotner, M.; Hunter, E.; Field, F. *J. Am. Chem. Soc.* **1979**, *101*, 686.
(37) Clarkson, J. R.; Dian, B. C.; Moriggi, L.; DeFusco, A.; McCarthy, V.; Jordan, K. D.; Zwier, T. S. *J. Chem. Phys.* **2005**, *122*, 214311.
(38) Guidi, M. *Spectroscopy and Dissociation Dynamics of Cold, Biomolecular Ions*. Ph.D. Thesis; Ecole Polytechnique Fédérale de Lausanne: 2009.
(39) Leroy, E.; Lami, H.; Laustria, G. *Photochem. Photobiol.* **1971**, *13*, 411.
(40) Rzeska, A.; Stachowiak, K.; Malicka, J.; Lankiewicz, L.; Wiczk, W. *J. Photochem. Photobiol., A* **2000**, *133*, 33.
(41) Bent, D.; Hayon, E. *J. Am. Chem. Soc.* **1975**, *97*, 2606.
(42) Hashimoto, T.; Takasu, Y.; Yamada, Y.; Ebata, T. *Chem. Phys. Lett.* **2006**, *421*, 227.
(43) Hickman, C.; Gascooke, J.; Lawrance, W. *J. Chem. Phys.* **1996**, *104*, 4887.
(44) Jacon, M.; Lardeux, C.; Lopezdelgado, R.; Tramer, A. *Chem. Phys.* **1977**, *24*, 145.
(45) Burton, C.; Noyes, W. *J. Chem. Phys.* **1968**, *49*, 1705.
(46) Dietz, T.; Duncan, M.; Smalley, R. *J. Chem. Phys.* **1982**, *76*, 1227.
(47) Lohmannsroben, H.; Luther, K.; Stuke, M. *J. Phys. Chem.* **1987**, *91*, 3499.
(48) Prochorow, J.; Hopewell, W.; El-Sayed, M. A. *Chem. Phys. Lett.* **1979**, *65*, 410.
(49) Huang, C.; Jiang, J.; Lee, Y.; Ni, C. *J. Chem. Phys.* **2002**, *117*, 7034.
(50) Huang, C.; Dyakov, Y.; Lin, S.; Lee, Y.; Ni, C. *J. Phys. Chem. A* **2005**, *109*, 4995.
(51) Tseng, C.-M.; Lin, M.-F.; Yang, Y. L.; Ho, Y. C.; Ni, C.-K.; Chang, J.-L. *Phys. Chem. Chem. Phys.* **2010**, *12*, 4989.
(52) Guidi, M.; Lorenz, U. J.; Papadopoulos, G.; Boyarkin, O. V.; Rizzo, T. R. *J. Phys. Chem. A* **2009**, *113*, 797.
(53) Zabuga, A.; Kamrath, M. Z.; Boyarkin,, O. V.; Rizzo, T. R. *J. Chem. Phys.* **2014**, in press.
(54) El Aribi, H.; Orlova, G.; Hopkinson, A.; Siu, K. *J. Phys. Chem. A* **2004**, *108*, 3844.
(55) Palmer, I.; Ragazos, I.; Bernardi, F.; Olivucci, M.; Robb, M. *J. Am. Chem. Soc.* **1993**, *115*, 673.